Available online at www.sciencedirect.com

ScienceDirect

IFAC Papers Online CONFERENCE PAPER ARCHIVE

IFAC PapersOnLine 50-1 (2017) 13834–13840

A New Scheme for Haptic Shared Lateral Control in Highway Driving Using Trajectory Planning

Mohamed Amir Benloucif, Anh-Tu Nguyen, Chouki Sentouh, Jean-Christophe Popieul

LAMIH, UVHC-CNRS UMR 8201, University of Valenciennes, France.
E-mails: {mohamed.benloucif, chouki.sentouh, jean-christophe.popieul}@univ-valenciennes.fr, nguyen.trananhtu@gmail.com

Abstract: Conflicts between the driver and systems for automated steering are important issues that affect the safety of the driver and the acceptability of the system. This paper presents a new framework for shared lateral control on highway driving using trajectory planning. The core idea of this work is to account for the driver's steering torque in the trajectory planning level in order to adjust the system's desired trajectory in a way that better suits the driver intention. By doing so, the system would strive towards the position aimed by the driver thus helping him to swerve within the lane with reduced effort and conflicting torques. The advantage of the proposed approach is demonstrated on a driving simulator study with a scenario of avoiding obstacles undetected by the system.

Keywords: Human-machine cooperation, shared control, lane keeping systems, trajectory planning, fuzzy model-based control.

1. INTRODUCTION

The last decade has seen great advances towards automated driving. Intensive research investigations have yielded numerous systems for advanced driver assistance. Although the ultimate goal is to achieve fully autonomous driving, many challenges remain unsolved and this technology still needs time to mature. In the meantime, many organisations such as the NHTSA (National Highway Traffic Safety Administration) and the OICA (International Organisation of Motor Vehicle Manufacturers) have proposed taxonomies defining the intermediate levels of automation Blanco et al. (2015). The levels currently being tackled consider only partial automation where the system controls the vehicle while the driver remains responsible for the driving task. Therefore, the driver's role has been shifted from control to supervision. Numerous studies in the literature have pointed out that the human factor issues arising from automation can be critical to the driver's safety Saffarian et al. (2012). In fact, one of the key issues in this kind of setups is the design of an appropriate driver-machine interaction as the acceptance of the developed system fully depends on it. In this framework, research on human-machine cooperation aims to lay down guidelines for designing effective human-machine systems. Interaction and interference management are at the heart of cooperation Hoc and Lemoine (1998). Since the driving task is hierarchically structured in three levels (strategic, tactical and operational) Michon (1985), such managements need to be addressed at each level. Cooperation at the tactical level boils down to cooperatively choosing the manoeuvre to execute. When the driver and the system come to conflicting decisions, an arbitration is crucial to attribute the final decision authority Benloucif et al. (2016a). On the operational level, a conflict can appear when the driver's control behavior is different than that of the system, for instance in curve negotiation or if the driver's preferred position on the lane is shifted from the lane centre. Another example of the conflict at this level is when the driver swerves from the lane centre to avoid a deteriorated portion of the road or an undetected obstacle. This case is more challenging for the driver's safety. As shown in Griffiths and Gillespie (2005), driving with an automated system that keeps the vehicle in the lane centre significantly decreases the obstacle avoidance. This raises the question of authority management between the system and the driver, and different ways to tackle this issue exist in the literature. For example, the authors in Cerone et al. (2009) have proposed a control strategy where the control loop is always active without requiring any switching strategy. However, this method can only guarantee either manual or automatic steering modes. This has motivated the introduction of haptic shared control approaches for lane keeping systems, which allow both the driver and the automation to steer *simultaneously* while they interact throughout the steering wheel. This fact has been reported to have many benefits regarding the driver's workload and performance Mulder et al. (2012). One category of haptic shared control considers a static degree of sharing as described in Abbink et al. (2012). The second aims to offer a sharing degree that adapts to the situation. High level information, like the driver's state, is used to model the driver's authority which is directly accounted for in the control scheme as proposed in Sentouh et al. (2013); Nguyen et al. (2016a, 2015). Therefore, in case of a conflict between the driver and the system, the latter reduces or increases its intervention according to the control authority given to the driver in that situation. As shown in Benloucif et al. (2016b), introducing the cooperation at the planning level not only reduces the system's opposing torques but also yields a beneficial assistance to reduce the steering effort of the driver.

This paper exploits the idea of adapting the trajectory according to the driver's control input proposed in Brandt et al. (2007) for shared lateral control purposes. We present a method to

10.1016/j.ifacol.2017.08.2223

account for the driver's torque to predict his/her desired lateral displacement which is then used to adjust accordingly the trajectory. The core idea here is to achieve haptic shared control by accounting for the driver's steering torque in the trajectory planning level. The system plans the vehicle trajectories that match the driver's intentions to help solving the upcoming conflicts. As a consequence, the system strives towards the position aimed by the driver thus helping him/her to swerve within the lane with reduced effort and negative interferences. Also, it allows the driver to choose a preferred position in the lane rather than the lane centre as proposed by all available assistance systems. The control method proposed in Nguyen et al. (2016b) is used to design a robust controller which can guarantee several control objectives. First, the controller can track effectively the planned trajectory in the presence of vehicle speed variation and unknown road curvatures. Second, the actuator saturation of the steering system can be explicitly taken into account in the control design to improve the the security and the confort of the passagers, for example the driver can override the system in some emergency driving situations.

The paper is organized as follows. Section 2 shows the global architecture of the proposed system. Section 3 details the trajectory planning algorithm for shared control and the method for predicting the driver's desired lateral movement. The used controller for trajectory tracking is discussed in Section 4. In Section 5, a driving simulator study is conducted for a scenario that illustrates a conflicting situation. Section 6 provides some concluding remarks and future works. Throughout this paper, the time argument is dropped when convenient.

2. SYSTEM OVERVIEW

The system architecture is depicted in Fig. 1, which is aimed for shared lateral control on highways. Therefore, the proposed system performs two main driving tasks, namely lane keeping and lane change.

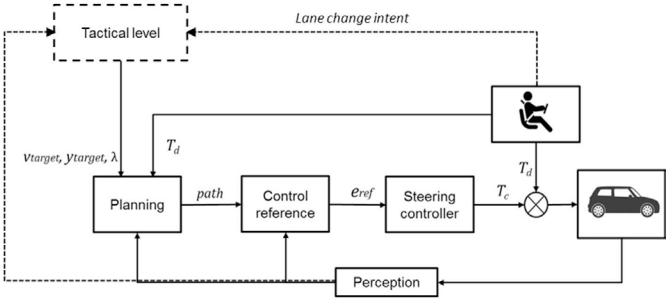

Fig. 1. Overview of the proposed shared lateral control.

The trajectory planning framework provides trajectories to guide the vehicle within the lane (lane keeping) or to execute lane change manoeuvres. The tactical level concerns the decision to change lanes when suited or when requested by the driver. It feeds the trajectory planner with information about the position of the desired lane centre y_{ref} and the desired velocity v_{ref}. The decision making process for lane changes is out of the scope of the paper.

The term shared control in this work targets the cooperation at the operational level. We apply it in our studied case to help the driver guide the vehicle and swerve within the same lane. In the absence of driver's steering commands, the system controls the vehicle along the initially planned trajectory. If the driver applies torques to steer away from the current position, the planned trajectory is updated. Given the importance of authority management when conflicts appear, we introduce the variable λ to arbitrate between the driver and the system. When the driver has the authority (he/she is not detected to be distracted for example), he/she would be allowed to alter the trajectory locally (within the lane).

The steering controller then simply tracks the planned trajectories and continuously acts on the steering wheel along with the driver as the appearing conflicts are managed upstream at the trajectory level. Also, the synthesized controller guarantees torque saturation so that the system can be overridden if the conflicts are not solved by the replanned trajectory. More details on the different components are given further in the paper.

3. TRAJECTORY PLANNING FOR SHARED CONTROL

Many trajectory planning approaches for automotive applications are available in the literature. An important requirement of the application in this work is the fast replanning frequency. Indeed, it is crucial to quickly account for the driver's changing torque to get a good haptic interaction instead of lags in the replanned trajectories. The latter might lead to confusion and increase torque conflicts.

Approaches that discretize the search space and execute an exhaustive search to find the optimal trajectory have already been used in real-time applications McNaughton et al. (2011). Glaser et al. (2010) presented a fast trajectory planning algorithm, which is implementable on an engine control unit with limited resources. The method referred to as hierarchical trajectory planning combines a behavioral layer which restrains the search space according to the driving context with a low level planner that determines the optimal trajectory within. Werling et al. (2012) proposed a real-time algorithm quiet similar in spirit where separate sets of longitudinal and lateral trajectories are evaluated and the best one is picked. This work inspired the trajectory planning algorithm adapted for haptic shared control.

3.1 Trajectory Planning Method

Polynomial path primitives have been widely used for local planning on structured environments like highways. It was shown in Takahashi et al. (1989) that fifth-order polynomials belong to the class of functions which constrain the jerk and guarantee jerk optimal trajectories. High order polynomials particularly provide optimised paths that ensure continuous velocities, accelerations and curvatures. They also allow a simple formulation of the planning problem which is presented as a boundary condition problem: find a smooth path that guides the vehicle from the initial state to the final state Papadimitriou and Tomizuka (2003). For the lateral movement, the initial state is the current lateral position, velocity and acceleration $[y_0\ \dot{y}_0\ \ddot{y}_0]$. With the assumption that the vehicle aims to travel towards the final lateral position y_f with a zero lateral velocity and acceleration, the final state is given by: $[y_f\ 0\ 0\ \mathcal{T}_y]$ where $\mathcal{T}_y$ is the lateral completion time. The lateral movement is then defined by a fifth-order polynomial time description. For the longitudinal movement, and as the final longitudinal position is not known, a fourth-order polynomial is derived to describe the vehicle longitudinal movement from the initial state $[x_0\ \dot{x}_0\ \ddot{x}_0]$ towards the final state $[\dot{x}_f\ 0\ \mathcal{T}_x]$ where the final velocity is the reference velocity and $\mathcal{T}_x$ is the longitudinal completion

time. Also we assume that the final acceleration is zero. The trajectories are then described by the following equations:

$$\begin{aligned} x(t) &= a_0 + a_1 t + a_2 t^2 + a_3 t^3 + a_4 t^4 \\ y(t) &= b_0 + b_1 t + b_2 t^2 + b_3 t^3 + b_4 t^4 + b_5 t^5 \end{aligned} \tag{1}$$

The polynomial coefficients are then trivially derived by solving the following equation system:

$$\begin{aligned} [a_0\ a_1\ a_2\ a_3\ a_4] &= \mathbf{A}\,[(x_0\ \dot{x}_0\ \ddot{x}_0\ \dot{x}_f\ \ddot{x}_f)]^\top \\ [b_0\ b_1\ b_2\ b_3\ b_4\ b_5] &= \mathbf{B}\,[y_0\ \dot{y}_0\ \ddot{y}_0\ y_f\ \dot{y}_f\ \ddot{y}_f]^\top \end{aligned} \tag{2}$$

where $\mathbf{A}$, $\mathbf{B}$ are functions of the completion times, defined as

$$\mathbf{A} = \begin{bmatrix} 1 & 0 & 0 & 0 & 0 \\ 0 & 1 & 0 & 0 & 0 \\ 0 & 0 & 2 & 0 & 0 \\ 0 & 1 & 2\mathcal{T}_x & 3\mathcal{T}_x^2 & 4\mathcal{T}_x^3 \\ 0 & 0 & 2 & 6\mathcal{T}_x & 12\mathcal{T}_x^2 \end{bmatrix}$$

$$\mathbf{B} = \begin{bmatrix} 1 & 0 & 0 & 0 & 0 & 0 \\ 0 & 1 & 0 & 0 & 0 & 0 \\ 0 & 0 & 2 & 0 & 0 & 0 \\ 1 & \mathcal{T}_y & \mathcal{T}_y^2 & \mathcal{T}_y^3 & \mathcal{T}_y^4 & \mathcal{T}_y^5 \\ 0 & 1 & 2\mathcal{T}_y & 3\mathcal{T}_y^2 & 4\mathcal{T}_y^3 & 5\mathcal{T}_y^4 \\ 0 & 0 & 2 & 6\mathcal{T}_y & 12\mathcal{T}_y^2 & 20\mathcal{T}_y^3 \end{bmatrix} \tag{3}$$

We note from (2) and (3) that a polynomial trajectory is defined by the initial state, the aimed final state and the completion time $\mathcal{T}_x$ and $\mathcal{T}_y$. The planning procedure is executed cyclically and in order to ensure the continuity of the trajectories, the initial state is always chosen from the previously calculated trajectory. The final states for both the longitudinal and lateral trajectories are chosen following the concept of discretized target manifolds presented in Werling et al. (2012). Therefore, a set of trajectories that swerve from and back towards the reference lateral position and reference velocity are evaluated.

For the lateral movement and as the trajectory planning algorithm is intended to handle both shared control (swerving within the lane limits) and lane changes (at the tactical level), a set of trajectories that lead to discretized lateral positions around the centre of the desired lane (y_{ref}) are evaluated according to multiple criteria as shown in Fig. 2. The set of lateral trajectories that share the same initial state is then constructed by combining different end conditions. The final states $[y_{fi}\ 0\ 0\ \mathcal{T}_{yj}]$ are given by

$$\begin{aligned} y_{fi} &= y_{ref} + \Delta y_i, \qquad \Delta y_i \in [-\Delta y_{\lim}, \Delta y_{\lim}] \\ \mathcal{T}_{yj} &= \mathcal{T}_{\min} + j\Delta\mathcal{T}, \qquad j = \{1, ..., M\} \end{aligned} \tag{4}$$

where Δy_i is the deviation from the lane center, $\Delta y_{\lim}$ is the maximum deviation and is chosen within to the lane limits, $\mathcal{T}_{\min}$ is the minimum completion time considered, $\Delta\mathcal{T}$ is the time step and M is related to the maximum trajectory length. The same concept is applied for the longitudinal trajectories but with a set of velocities around the target speed y_{ref} instead.

For autonomous driving, the evaluation of the trajectories is performed regarding the produced jerk, the time of completion and the relative lateral position (respect. speed) to the reference position (respect. speed) for the lateral (respect. longitudinal) movement. The idea is to penalize the slowly convergent trajectories and those falling far from the reference position (respect. reference speed). The cost functions are given as

$$\begin{aligned} \mathbb{C}_x &= k_j \mathbf{J_x} + k_t \mathcal{T}_x + k_v (v_x - v_{ref})^2 \\ \mathbb{C}_y &= k_j \mathbf{J_y} + k_t \mathcal{T}_y + k_y (y - y_{ref})^2 \end{aligned} \tag{5}$$

with

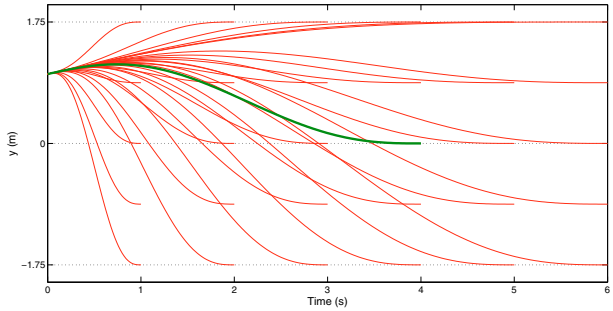

Fig. 2. Construction and evaluation of a set of lateral trajectories ($\Delta y_{\lim} = 1.75$ and $\Delta\mathcal{T} = 1s$).

$$\mathbf{J_x} = \int_0^{\mathcal{T}_x} \dddot{x}^2(\tau) d\tau, \quad \mathbf{J_y} = \int_0^{\mathcal{T}_y} \dddot{y}^2(\tau) d\tau$$

where $\mathbb{C}_x$ and $\mathbb{C}_y$ are the cost functions for the longitudinal and lateral trajectories and $\mathbf{J_x}$, $\mathbf{J_y}$ are the integral of the squared jerk cost term for both trajectory components. The coefficients k_j, k_t, k_v and k_y represent respectively the weights for the jerk, time, relative speed and relative lateral position cost terms. The trajectory minimizing the cost function is to be chosen.

The following expressions of the polynomial trajectories allow us to *analytically* compute the jerk cost term only considering the polynomial coefficients and the time of completion $\mathcal{T}_x$ or $\mathcal{T}_y$ without having to compute the explicit trajectory points:

$$\begin{aligned} \mathbf{J_x} &= 36[a_3^2 \mathcal{T}_x + 4a_3 a_4 \mathcal{T}_x^2 + \frac{16}{3} b_4^2) \mathcal{T}_x^3] \\ \mathbf{J_y} &= 36[b_3^2 \mathcal{T}_y + 4b_3 b_5 \mathcal{T}_y^2 + (\frac{20}{3} b_3 b_5 + \frac{16}{3} b_4^2) \mathcal{T}_y^3 \\ &\quad ... + 20 b_4 b_5 \mathcal{T}_y^4 + 20 b_5^2 \mathcal{T}_y^5] \end{aligned} \tag{6}$$

It is then possible to evaluate effectively the set of trajectories and only the best one is sampled. The generated trajectory is then checked for outsized accelerations and curvature to exclude the uncomfortable and unfeasible ones. If a trajectory is invalidated, the next best ranked one is sampled and the checking procedure is revaluated. This procedure decreases the time and memory resources needed by the trajectory planning algorithm.

3.2 Desired Lateral Displacement Prediction

In order to adjust the planned trajectory to the driver's intention, it is important to predict the desired lateral position. The latter is hard to predict based on the current measured steering wheel angle, as used in Brandt et al. (2007), since it is the result of the summation of both the driver's and the system's torques. For this matter we propose to first isolate the influence of the driver's torque on the dynamics of the vehicle and predict the vehicle trajectory as if the system was not acting on steering wheel. Using a transfer function, the yaw rate that would have been generated only by the driver's torque is obtained. The transfer function is based on the bicycle model augmented with the steering column model, see Section 4. The deduced yaw rate is then used along with the vehicle velocity as an input of a vehicle motion model to predict the lateral position on a time horizon as shown in Fig. 3. The vehicle model used here is the constant turn rate and velocity (CTRV) model, depicted in Fig. 4, which is widely used for prediction and tracking applications Koller et al. (1993). This model assumes a stationary case where the vehicle performs a circular motion

with a constant magnitude of the translational velocity v_x and a constant angular velocity corresponding to the yaw rate r. The remaining three state variables describing the vehicle are the vehicle center coordinates x_g, y_g and the yaw angle ψ.

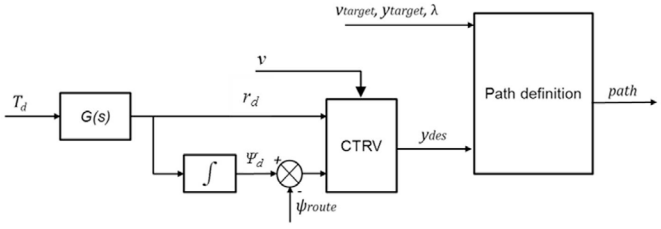

Fig. 3. Prediction of the driver's desired lateral displacement.

Let us define the vehicle state vector

$$X(t) = [x_g(t)\ y_g(t)\ \psi(t)\ v(t)\ r(t)]^\top,$$

the evolution of the model is described by the following non-linear state transition equations:

$$X(t+\mathcal{T}) = \begin{cases} x_g(t) + \mu(t)(r(t)\mathcal{T} + \sin(\psi(t)) - \sin(\psi(t))) \\ y_g(t) + \mu(t)(r(t)\mathcal{T} - \cos(\psi(t)) + \sin(\psi(t))) \\ \psi(t) + r(t)\mathcal{T} \\ v(t) \\ r(t) \end{cases} \tag{7}$$

where $\mu(t) = v(t)/r(t)$. The value of the prediction horizon $\mathcal{T}$ is important for the effectiveness of the approach. A too small prediction horizon leads to a predicted trajectory very close to the actual one and therefore it would not be useful to adapt the planned trajectory. A too large horizon leads to overshoots for the predicted trajectory and the instability for the planned trajectories as the system becomes too sensitive to the driver's torque. Finally, the choice of the prediction horizon was done experimentally to get a good steering feeling and was set to $\mathcal{T} = 1s$. From the predicted desired lateral displacement, the desired lateral position of the driver is given by

$$y_d = y_g + \Delta y_d(t_p) \tag{8}$$

where $\Delta y_d(t_p)$ is the predicted desired lateral displacement, see Fig. 4. The illustration result of the prediction method for a lateral displacement of $1.75m$ is shown in Fig. 5.

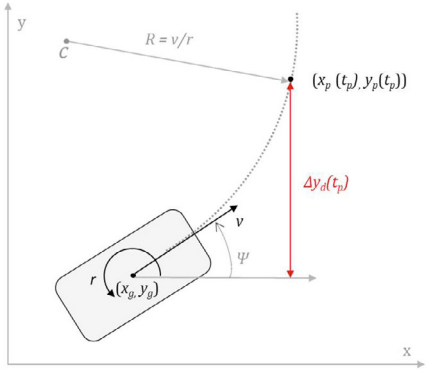

Fig. 4. CTRV model and lateral desired displacement prediction in a horizon t_p.

3.3 Integration of Driver's Actions in the Trajectory Planning

The variable λ, provided by the Tactical level, characterizes the authority of the driver in altering the planned trajectory.

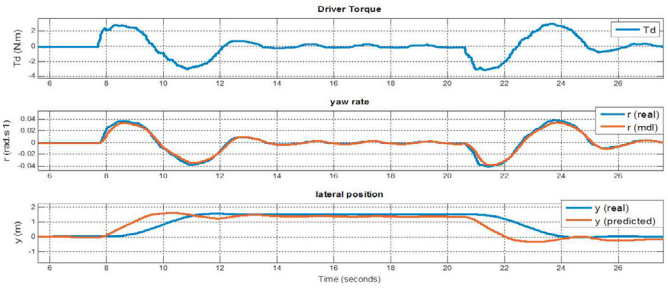

Fig. 5. Predicted lateral position for a lateral displacement of $1.75m$ ($t_p = 1s$).

In Sentouh et al. (2013), the driver authority is modeled as a smoothed binary variable that tends to 1 when the conflict between the driver and the assistance torques exceeds a certain threshold. Additional information can be used, such as the driver's state, to reject the intervention of the driver in case of distraction Nguyen et al. (2016a). Here, we model λ in such a way that the system ignores the driver's desired lateral position when his/her torque is negligible or when he/she is detected to be distracted. The variable λ, illustrated in Fig. 6 (a), is expressed as follows:

$$\lambda = DS\left(1 - e^{-\varepsilon|T_d|}\right) \tag{9}$$

where DS represents the distraction state ($DS = 1$ if the driver is not distracted and 0 otherwise), T_d is the driver torque and ϵ is a scaling factor. The information on the driver distraction is provided by a driver monitoring system.

We note that the cost function related to the longitudinal trajectories remains the same as in (5). However, the one evaluating the lateral trajectories becomes

$$\begin{aligned} \mathbb{C}_y &= k_j \mathbf{J_y} + k_t \mathcal{T} + k_y (y - y_{ref})^2 + \lambda k_d g(y, y_{des}) \\ g(y, y_{des}) &= 1 - 1/\cosh\left(\sigma(y - y_{des})\right) \end{aligned} \tag{10}$$

where k_d represents the weight for the driver's cost term, $g(\cdot)$ is the cost functional for the driver's desired lateral position, and the scaling factor σ is chosen such that $g(\cdot)$ tends to zero narrowly around y_{des} to give more importance towards the driver's desired lateral position as depicted in Fig. 6 (b).

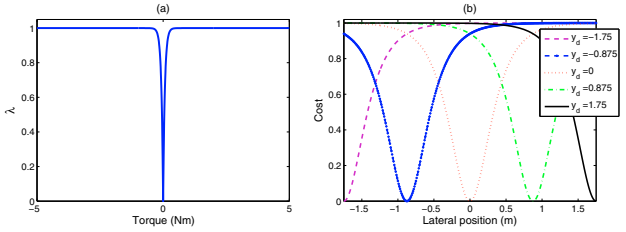

Fig. 6. (a) Driver authority with $\epsilon = 15$. (b) Driver cost function according to different desired lateral positions ($\sigma = 4$).

4. ROBUST CONTROL FOR TRAJECTORY TRACKING

4.1 Vehicle Control-Based Model

For control purposes, the road-vehicle model is derived from the bicycle vehicle model augmented with the lane keeping dynamics and the steering system, expressed as follows:

$$\dot{x}(t) = A_v x(t) + B_v u(t) + E_v w(t) \tag{11}$$

where the state vector $x = \left[\beta\ r\ \psi_L\ y_L\ \delta\ \dot{\delta}\right]^\top$ is composed by the sideslip angle β, the yaw rate r, the heading error ψ_L,

the lateral offset y_L from the road centerline at a look-ahead distance l_s. The disturbance vector $w = [f_w \ \rho_r]^\top$ is composed of the wind force f_w and the road curvature ρ_r. The control input is the total steering torque $u = T_s$. The system matrices of the vehicle model (11) are given by

$$A_v = \begin{bmatrix} a_{11} & a_{12} & 0 & 0 & b_1 & 0 \\ a_{21} & a_{22} & 0 & 0 & b_2 & 0 \\ 0 & 1 & v_x & 0 & 0 & 0 \\ v_x & l_s & v_x & 0 & 0 & 0 \\ 0 & 0 & 0 & 0 & 0 & 1 \\ a_{61} & a_{62} & 0 & 0 & a_{65} & a_{66} \end{bmatrix}, \quad E_v = \begin{bmatrix} e_1 & 0 \\ e_2 & 0 \\ 0 & -v_x \\ 0 & 0 \\ 0 & 0 \\ 0 & 0 \end{bmatrix}$$

$$B_v = \begin{bmatrix} 0 & 0 & 0 & 0 & 0 & \dfrac{1}{R_s I_s} \end{bmatrix}^\top$$

where

$$a_{11} = -\frac{2(C_f + C_r)}{m v_x}, \ a_{12} = \frac{2(l_r C_r - l_f C_f)}{m v_x^2} - 1,$$
$$a_{21} = \frac{2(l_r C_r - l_f C_f)}{I_z}, \ a_{22} = \frac{-2(l_r^2 C_r + l_f^2 C_f)}{I_z v_x},$$
$$b_1 = \frac{2C_f}{m v_x}, \ b_2 = \frac{2 l_f C_f}{I_z}, \ e_1 = \frac{1}{m v_x}, \ e_2 = \frac{l_w}{I_z},$$
$$a_{61} = \frac{2K_p C_f \eta_t}{R_s^2 I_s}, \ a_{62} = \frac{2K_p C_f \eta_t}{R_s^2 I_s} \frac{l_f}{v_x},$$
$$a_{65} = -\frac{2K_p C_f \eta_t}{R_s^2 I_s}, \ a_{66} = -\frac{B_s}{I_s}.$$

The values of the vehicle parameters are given in Table 1. To ease the control implementation, the Euler's approximation is used to derive the following discrete-time version of state-space representation Nguyen et al. (2016c):

$$x(k+1) = Ax(k) + B_u u(k) + B_w w(k) \tag{12}$$

where $A = I + \mathcal{T}_e A_v$, $B_u = \mathcal{T}_e B_v$, $B_w = \mathcal{T}_e E_v$ and $\mathcal{T}_e$ is the sampling time. Note that the system matrices A, B_u, B_w are time-varying due to their dependency to the vehicle speed v_x. Moreover, as aforementioned the steering actuator saturation should be considered in the control design for security and confort reasons. Hereafter, we present design conditions to cope with these technical and practical control issues.

Table 1. Vehicle model parameters

Parameter	Description	Value
M	Total mass of the vehicle	2025 kg
l_f	Distance from the CG to front axle	1.3 m
l_r	Distance from the CG to rear axle	1.6 m
l_w	Distance from the CG to impact center of the wind force	0.4 m
l_s	Look-ahead distance	5 m
η_t	Tire length contact	0.13 m
I_z	Vehicle yaw moment of inertia	2800 kgm^2
I_s	Steering system moment of inertia	0.02 kgm^2
R_s	Steering gear ratio	16
B_s	Steering system damping	5.73
K_p	Manual steering column coefficient	0.5
C_f	Front cornering stiffness	57000 N/rad
C_r	Rear cornering stiffness	59000 N/rad

4.2 Robust Control Design

This section summarizes the robust control design proposed in Nguyen et al. (2016b), which is applied to track the desired trajectory for shared lateral control purposes. To this end, the vehicle system (12) is transformed into the following Takagi-Sugeno model while taking into account the control input saturation (see Nguyen et al. (2016c) for more details):

$$x(k+1) = \sum_{i=1}^{r} \eta_i(\theta) \left(A_i x(\kappa) + B_i^u \operatorname{sat}(u(\kappa)) + B_i^w w(\kappa) \right) \tag{13}$$

where θ is the premise vector (related to the vehicle speed) and r is the number of fuzzy model rules. The standard saturation function is defined as follows:

$$\operatorname{sat}\left(u_{(l)}\right) = \operatorname{sign}\left(u_{(l)}\right) \min\left(\left|u_{(l)}\right|, u_{\max(l)}\right), \ \ l = 1, \ldots, n_u.$$

The real matrices A_i, B_i^u, B_i^w, C_i, $i = 1, \ldots, r$, are constant and of adequate dimensions. Note that the normalized membership functions $\eta_i(\theta)$, $i = 1, \ldots, r$, satisfy the convex sum property. Assume that the disturbance w is bounded in amplitude, namely it belongs to the following class of function:

$$\mathcal{W}_\alpha^\infty = \left\{ w : \mathbb{R}^+ \to \mathbb{R}^{n_w}, \quad w^\top(\kappa) w(\kappa) \leq \alpha, \ \kappa \geq 0 \right\} \tag{14}$$

where the bound $\alpha > 0$ is given.

To stabilize the system (13), we make use of the following control law:

$$u(\kappa) = \left(\sum_{i=1}^{r} \eta_i(\theta) G_i \right) \left(\sum_{i=1}^{r} \eta_i(\theta) H_i \right)^{-1} x(\kappa) \tag{15}$$

where the control gains G_i and H_i, $i = 1, \ldots, r$, are designed with the following theorem.

Theorem 1. Given the system (13) where $w \in \mathcal{W}_\alpha^\infty$, and positive scalars α, $\tau_1 < 1$. If there exist positive definite matrices X_i, positive diagonal matrices S_i, matrices H_i, G_i, W_i of appropriate dimensions, $i = 1, \ldots, r$, and a positive scalar τ_2 such that

$$\begin{bmatrix} H_i + H_i^\top - X_i & \star \\ G_{i(l)} - W_{i(l)} & u_{\max(l)}^2 \end{bmatrix} > 0 \tag{16}$$

$$\tau_1 - \tau_2 \alpha > 0 \tag{17}$$

$$\Psi_{ii}^k < 0 \tag{18}$$

$$\frac{2}{r-1} \Psi_{ii}^k + \Psi_{ij}^k + \Psi_{ji}^k < 0 \tag{19}$$

for $i, j, k = 1, \ldots, r$, $l = 1, \ldots, n_u$ and $i < j$. The quantity Ψ_{ij}^k is defined as

$$\Psi_{ij}^k = \begin{bmatrix} (\tau_1 - 1)\left(H_i + H_i^\top - X_i\right) & \star & \star & \star \\ W_i & -2S_i & \star & \star \\ 0 & 0 & -\tau_2 I & \star \\ A_j H_i + B_j^u G_i & -B_j^u S_i & B_j^w & -X_k \end{bmatrix}.$$

Then, the controller (15) stabilizes the saturated system (13).

The reader can refer to Nguyen et al. (2016b,c) for the detailed proof of Theorem 1 and the computation of the control feedback gains using numerical solvers.

5. EXPERIMENTAL RESULTS

5.1 SHERPA Advanced Driving Simulator and Test Scenario

The study was carried out with the SHERPA-LAMIH driving simulator which is based on a Peugeot 206 mock-up fixed on a six-DOF motion system, see in Fig. 7. The simulator is equipped with an active steering wheel and sensors that provide steering angle, steering rate and steering torque. A force feedback gas pedal as well as a driver monitoring system, both provided by Continental Automotive, have been installed.

The visual is displayed on a $240°$ wide panoramic screen. Using the SCANeR environment, all control algorithms have been implemented in the SHERPA-LAMIH simulator through Matlab/Simulink software.

Fig. 7. SHERPA driving simulator.

To illustrate the proposed shared control concept, a short obstacle avoidance scenario has been examined. The drivers are instructed to stay in the lane and avoid twelve stopped vehicles placed on the track such that they obstruct partly the lane. Groups of four vehicles constitute a situation as shown in Fig. 8. Three situations distinguished by the spacing between vehicles are set respectively with a spacing of: $150m$, $100m$, $50m$. For the sake of the experiment, the obstacles are not detected by the system and the participant drivers are instructed to swerve within the lane to avoid collisions while driving at a fixed speed of $80km/h$. The data has been collected from 5 drivers. The participants tested three system settings with this scenario: (i) *Manual control*, (2) *No shared control* (the controller follows the lane centre only) and (iii) the proposed *Shared control*. The settings are tested in a randomized order.

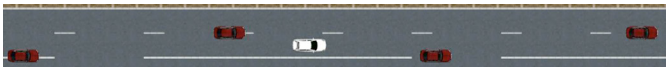

Fig. 8. Driving test scenario.

5.2 Experimental Results and Discussions

As an example, the results obtained with the first participant are shown in Figs. 9, 10 and 11.

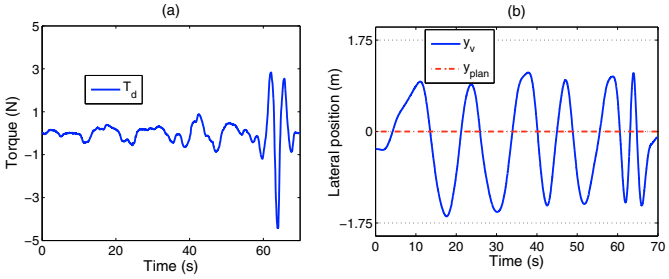

Fig. 9. Results of *Manual control*.

Observe from Figs. 9, 10 and 11 (a) that as three situations carry on, the driver torque increases to avoid the obstacles as the manoeuvres become more severe. Compared to *Manual control* shown in Fig. 9 (a), the driver's torque in *No shared control* setting is much larger during the whole scenario, see Fig. 10 (a). We can also see that the assistance torque T_a (in red) is always opposed to the driver's actions as he swerves from the lane

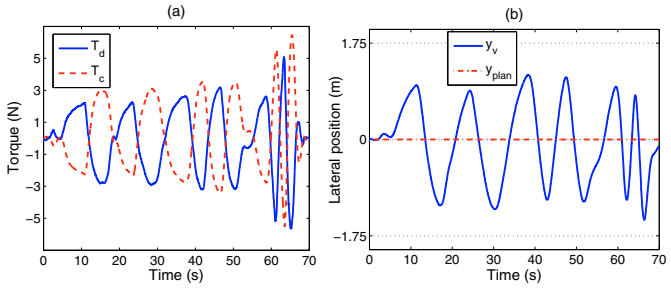

Fig. 10. *No shared control*: (a) driver and assistance torques, (b) vehicle lateral position against the planned trajectory.

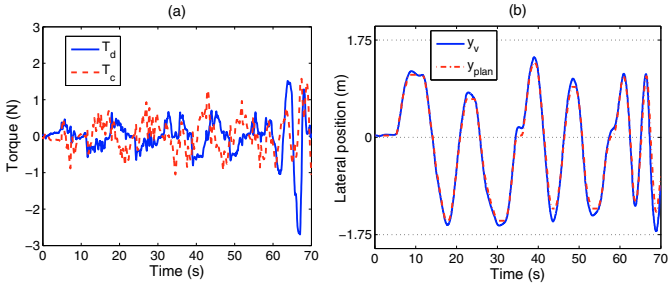

Fig. 11. *Shared control*: (a) driver and assistance torques, (b) vehicle lateral position against the planned trajectory.

centre, since the driver and the system have conflicting control objectives, see Fig. 10 (b). In contrast, Fig. 11 (a) shows that the driver torque with *Shared control* setting is in the same range as in the case of *Manual control*. Also, the assistance torque is less opposed to the driver actions. This is explained in Fig. 11 (b), which shows how the planned trajectories (in red) match the real trajectory. Hence, when the controller tracks the planned trajectories, it was helping the driver to achieve the avoidance manoeuvres. However, note that the planned trajectories remain within the current lane. This means that when approaching the lane border the driver action would be countered as long as the intent for a lane change is not expressed (turn indicator for instance).

For an objective comparison of the different settings, four indicators have been used. The two first ones are used to evaluate the steering feeling and comfort: (i) the time consistency (the time ratio where the assistance steers in the same direction as the driver) over the total scenario duration, (ii) the effort consistency (the ratio of the beneficial assistance effort over the total assistance effort delivered during the scenario). The two other indicators concern the total driver steering effort over the scenario and the steering resistance of the assistance, defined as

$$ST_{effort} = \int_0^{\mathcal{T}_{sc}} T_d^2(\tau)d\tau, \quad ST_{resist} = \int_{\mathcal{T}_r} T_d^2(\tau)d\tau \qquad (20)$$

where $\mathcal{T}_{sc}$ is the duration of the scenario and $\mathcal{T}_r$ is the total duration where $T_a T_d < 0$. Naturally, these metrics at the exception of the steering effort are not relevant for the *Manual control* case since they evaluate the interactions between the driver and the assistance. The mean over the results of five drivers are reported in Fig. 12. As depicted in Fig 12 (a), when the system does not share the control, the effort needed to steer the car and to avoid the obstacles is very large compared to *Manual control*. However, with *Shared control* the effort is low and in the same range as *Manual control* since the system

assists the driver during the manoeuvres. It is clear from Fig. 12 (b) that the system significantly reduces its resistance with *Shared control*. Finally, Figs. 12 (c) and (d) show a significant increase in the assistance consistency regarding to the driver's actions with *Shared control* compared to the classic case.

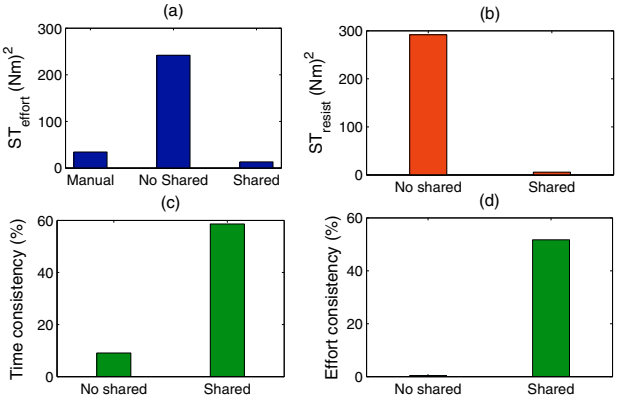

Fig. 12. Comparison between three control settings.

6. CONCLUSION

A new scheme for shared lateral control for highway application has been introduced. In contrast to the existing works, the goal is not only to reduce the conflicts but to help solving them by providing a positive assistance. To this end, the cooperation is directly accounted for at the planning level. The preliminary results obtained with the SHERPA driving simulator and human drivers are promising. In a near future, the proposed shared control approach need still to be studied more thoroughly in user tests for validation.

REFERENCES

Abbink, D.A., Mulder, M., and Boer, E.R. (2012). Haptic shared control: smoothly shifting control authority? *Cognition, Technology & Work*, 14(1), 19–28.

Benloucif, M., Popieul, J.C., and Sentouh, C. (2016a). Multi-level cooperation between the driver and an automated driving system during lane change maneuver. In *IEEE Intelligent Vehicles Symposium*, 1224–1229.

Benloucif, M.A., Popieul, J.C., and Sentouh, C. (2016b). Architecture for multi-level cooperation and dynamic authority management in an automated driving system - a case study on lane change cooperation. *IFAC-PapersOnLine*, 49(19), 615–620.

Blanco, M., Atwood, J., Vasquez, H.M., Trimble, T.E., Fitchett, V.L., Radlbeck, J., and Morgan, J.F. (2015). Human factors evaluation of level 2 and level 3 automated driving concepts. Technical Report No. DOT HS 812 182, Washington, DC: National Highway Traffic Safety Administration.

Brandt, T., Sattel, T., and Bohm, M. (2007). Combining haptic human-machine interaction with predictive path planning for lane-keeping and collision avoidance systems. In *IEEE Intelligent Vehicles Symposium*, 582–587.

Cerone, V., Milanese, M., and Regruto, D. (2009). Combined automatic lane-keeping and driver's steering through a 2-DOF control strategy. *IEEE Transactions on Control Systems Technology*, 17(1), 135–142.

Glaser, S., Vanholme, B., Mammar, S., Gruyer, D., and Nouveliere, L. (2010). Maneuver-based trajectory planning for highly autonomous vehicles on real road with traffic and driver interaction. *IEEE Transactions on Intelligent Transportation Systems*, 11(3), 589–606.

Griffiths, P.G. and Gillespie, R.B. (2005). Sharing control between humans and automation using haptic interface: primary and secondary task performance benefits. *Journal of the Human Factors and Ergonomics Society*, 47(3), 574–590.

Hoc, J.M. and Lemoine, M.P. (1998). Cognitive evaluation of human-human and human-machine cooperation modes in air traffic control. *The International Journal of Aviation Psychology*, 8(1), 1–32.

Koller, D., Daniilidis, K., and Nagel, H.H. (1993). Model-based object tracking in monocular image sequences of road traffic scenes. *International Journal of Computer Vision*, 10(3), 257–281.

McNaughton, M., Urmson, C., Dolan, J.M., and Lee, J.W. (2011). Motion planning for autonomous driving with a conformal spatiotemporal lattice. In *IEEE International Conference on Robotics and Automation (ICRA)*, 4889–4895.

Michon, J.A. (1985). A critical view of driver behavior models: what do we know, what should we do? In *Human Behavior and Traffic Safety*, 485–524. Springer.

Mulder, M., Abbink, D.A., and Boer, E.R. (2012). Sharing control with haptics seamless driver support from manual to automatic control. *Human Factors: The Journal of the Human Factors and Ergonomics Society*, 54(5), 786–798.

Nguyen, A.T., Sentouh, C., and Popieul, J.C. (2016a). Driver-automation cooperative approach for shared steering control under multiple system constraints: Design and experiments. *IEEE Transactions on Industrial Electronics*, PP(99), 1–1. doi:10.1109/TIE.2016.2645146.

Nguyen, A.T., Laurain, T., Palhares, R., Lauber, J., Sentouh, C., and Popieul, J.C. (2016b). LMI-based control synthesis of constrained Takagi-Sugeno fuzzy systems subject to $\mathcal{L}_2$ or $\mathcal{L}_\infty$ disturbances. *Neurocomputing*, 207, 793–804.

Nguyen, A.T., Sentouh, C., and Popieul, J.C. (2016c). Takagi-sugeno model-based steering control for autonomous vehicles with actuator saturation. *IFAC-PapersOnLine*, 49(5), 206–211.

Nguyen, A.T., Sentouh, C., Popieul, J.C., and Soualmi, B. (2015). Shared lateral control with online adaptation of the automation degree for driver steering assist system: A weighting design approach. In *54th Annual Conference on Decision and Control*, 857–862. Osaka, Japan.

Papadimitriou, I. and Tomizuka, M. (2003). Fast lane changing computations using polynomials. In *Proc. of the 2003 American Control Conference*, volume 1, 48–53.

Saffarian, M., de Winter, J.C., and Happee, R. (2012). Automated driving: human-factors issues and design solutions. In *Proc. of the Human Factors and Ergonomics Society Annual Meeting*, volume 56, 2296–2300.

Sentouh, C., Soualmi, B., Popieul, J.C., and Debernard, S. (2013). Cooperative steering assist control system. In *IEEE International Conference on Systems, Man, and Cybernetics*, 941–946. Manchester, UK. doi:10.1109/SMC.2013.165.

Takahashi, A., Hongo, T., Ninomiya, Y., and Sugimoto, G. (1989). Local path planning and motion control for AGV in positioning. In *IEEE/RSJ International Workshop on Intelligent Robots and Systems*, 392–397. doi: 10.1109/IROS.1989.637936.

Werling, M., Kammel, S., Ziegler, J., and Gröll, L. (2012). Optimal trajectories for time-critical street scenarios using discretized terminal manifolds. *The International Journal of Robotics Research*, 31(3), 346–359.